

Adversarial Driving: Attacking End-to-End Autonomous Driving

Han Wu, Syed Yunas, Sareh Rowlands, Wenjie Ruan, and Johan Wahlstrom*

Abstract—As the research in deep neural networks advances, deep convolutional networks become feasible for automated driving tasks. There is an emerging trend of employing end-to-end models in the automation of driving tasks. However, previous research unveils that deep neural networks are vulnerable to adversarial attacks in classification tasks. While for regression tasks such as autonomous driving, the effect of these attacks remains rarely explored. In this research, we devise two white-box targeted attacks against end-to-end autonomous driving systems. The driving model takes an image as input and outputs the steering angle. Our attacks can manipulate the behavior of the autonomous driving system only by perturbing the input image. Both attacks can be initiated in real-time on CPUs without employing GPUs. This research aims to raise concerns over applications of end-to-end models in safety-critical systems.

I. INTRODUCTION

Autonomous Driving is one of the most challenging tasks in safety-critical robotic applications. Most real-world autonomous vehicles employ modular systems that divide the driving task into smaller subtasks. Recent advances in high-performance GPUs facilitate the development of photo-realistic driving simulators, such as the Carla Simulator [1] and the Microsoft Airsim Simulator [2]. Researchers can explore the potential of end-to-end driving systems without safety concerns in simulated environments. We see more and more publications about end-to-end deep learning models, but are we ready to embrace end-to-end driving models in the real world?

Both modular systems and end-to-end driving systems use deep neural networks. Modular systems consist of localization, perception, prediction, planning, and control. The perception module relies on deep learning models to locate and classify objects in the environment. On the other hand, the end-to-end driving system is a monolithic module that directly maps the input to the output. For example, the NVIDIA end-to-end driving model [3] maps raw pixels from a single front-facing camera to steering commands.

However, deep neural networks are vulnerable to adversarial attacks, thus putting both modular and end-to-end systems at threat. Goodfellow et al. fool an image classification model by adding a small perturbation to the input image [4]. Instead of minimizing the training loss, they maximize the training loss by updating the input image. The perturbation is unperceivable by human eyes, but the classifier produces incorrect labels.

Han Wu, Sareh Rowlands and Johan Wahlstrom are with the University of Exeter, Stocker Rd, Exeter EX4 4PY, the UK (hw630@exeter.ac.uk; s.rowlands@exeter.ac.uk; j.wahlstrom@exeter.ac.uk).

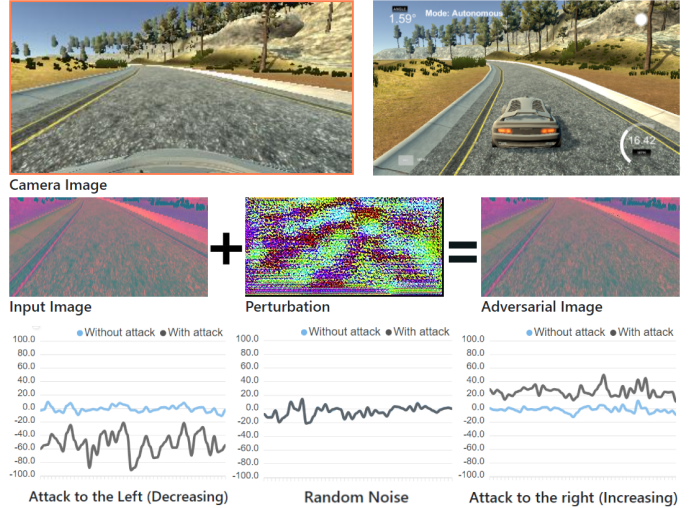


Fig. 1: Adversarial Driving: The behavior of the end-to-end autonomous driving model can be manipulated by adding unperceivable perturbations to the input image.

While end-to-end learning may lead to better performance and smaller systems, the monolithic module is vulnerable to adversarial attacks. Current research on adversarial attacks primarily focuses on classification tasks. The effect of these attacks on regression tasks largely remains unexplored. Our research explores the possibility of achieving real-time attacks against the NVIDIA end-to-end driving model, which is a regression model (see Figure 1).

Overall, the contributions of this paper are summarized as follows:

- We achieve a real-time online attack against the end-to-end regression model for autonomous driving. We validate our attacks in simulated environments and a real robot. The online attack demonstrates that we can deviate the vehicle in several seconds.
- We devise two white-box adversarial attacks against the regression model: one strong attack that generates the perturbation for each frame (image-specific); one weak attack that produces a universal adversarial perturbation that attacks all frames (image-agnostic).
- Our system is open-sourced on Github and can be extended to design more adversarial attacks for future research¹.

¹The code is available on Github: <https://github.com/wuhanstudio/adversarial-driving>

II. PRELIMINARIES

A. End-to-End Driving Systems

Recent advances in autonomous driving simulators stimulate the development of end-to-end driving systems. Modular systems divide the driving pipeline into submodules and employ end-to-end models in the perception module. On the other hand, end-to-end driving systems treat the entire driving pipeline as a monolithic module that maps sensor inputs directly to steering commands [5].

End-to-End driving systems consist of imitation learning and reinforcement learning methods. Imitation learning methods use deep neural networks to mimic human driving behavior. Reinforcement learning methods improve driving policies via exploration and exploitation. Though there is a growing trend of publications that use reinforcement learning, imitation learning is still the most popular one [6]. Our research focuses on attacking imitation learning models.

The first attempt at imitation-learning-based end-to-end driving system was the Autonomous Land Vehicle in a Neural Network (ALVINN) system, which trained a 3-layer fully connected network to steer a vehicle on public roads [7]. There are also applications of end-to-end off-road driving [8]. More recently, researchers from NVIDIA built a convolutional neural network to map raw pixels from a single front-facing camera directly to steering commands [3]. The NVIDIA end-to-end driving model is our target model, and we introduce model details in the next section.

B. Adversarial Attacks

Existing adversarial attacks can be categorized into white-box, gray-box, and black-box attacks [9]: In white-box attacks, the adversaries have full knowledge of the target model, including model architecture and parameters; In gray-box attacks, the adversaries have partial information about the target model; In black-box attacks, the adversaries can only gather information about the model through querying. We devise two white-box attacks that achieve real-time attacks against end-to-end driving models.

End-to-End driving models that use imitation learning are regression models that output continuous steering commands. However, prior research on adversarial attacks primarily focuses on attacking classification models.

Attacking a classification model: A successful attack against classification models deviates the output from the correct label. Taking the digital handwritten digit classification task as an example, an attacker can fool the classifier into recognizing the number 3 as 7.

Attacking a regression model: Adversarial attacks against regression models are more challenging. An attack that deviates the steering angle from 1.0 to 1.01 is unsuccessful because such a tiny deviation may not noticeably affect the driving outcome. As a result, a successful attack must drift the steering commands outside of a safe range. For example, we can use the Root Mean Square Error (RMSE) to evaluate an attack. A successful attack should produce a higher RMSE than random noises with the same total amount of disturbance [10] [11].

III. ADVERSARIAL DRIVING

This section formulates the problem, and then we introduce our target model and clarifies the differences between online and offline attacks. Furthermore, we devise two white-box attacks for our real-time online attack. Lastly, we present the architecture of the system.

A. Problem Formulation

Our objective is to fool an end-to-end driving model, which is a regression model. We use the following notations throughout the paper:

- x : The original input image.
- η : The adversarial perturbation.
- x' : The adversarial input image $x' = x + \eta$.
- y' : The adversarial output.
- y^* : The ground truth of the steering command.
- \hat{y} : The benign output of the steering command.
- $f(\theta, x)$: The regression model that maps input images to steering command. θ represents the parameters of the model. $\hat{y} = f(\theta, x)$ and $y' = f(\theta, x')$.
- $J(\hat{y}, y^*)$: The training loss used to train the model.

Given an input image x , the objective of attacking a classifier is to generate a small perturbation η , such that $y' \neq y^*$. But attacking a regression model requires the difference between y' and y^* to be larger than the average deviation δ caused by random noises, thus $y' - y^* > \delta$.

Besides, the perturbation should be unperceivable by human eyes, and we use the L_2 norm to measure the perturbation. In our experiments, $\xi = 0.03$.

$$\|x' - x\|_2 = \|\eta\|_2 \leq \xi \quad (1)$$

B. The End-to-End Driving Model

We use the NVIDIA end-to-end driving model as our target. The input shape of the model is (160, 320, 3), which represents (height, width, channel) respectively. The output steering angle is in the range of [-1, 1]. The output of -1 represents steering to the left, and the output of 1 means steering to the right.

| Layer | Output Shape | Parameters |
|---------|---------------------|------------|
| Input | (None, 160, 320, 3) | 0 |
| Conv2D | (None, 78, 158, 24) | 1824 |
| Conv2D | (None, 37, 77, 36) | 21636 |
| Conv2D | (None, 17, 37, 48) | 43248 |
| Conv2D | (None, 15, 35, 64) | 27712 |
| Conv2D | (None, 13, 13, 24) | 36928 |
| Dropout | (None, 13, 13, 24) | 0 |
| Flatten | (None, 27456) | 0 |
| Dense | (None, 100) | 2745700 |
| Dense | (None, 50) | 5050 |
| Dense | (None, 10) | 510 |
| Dense | (None, 1) | 11 |

TABLE I: The structure of the end-to-end driving model.

The input image is captured by the front camera, and then we apply predefined preprocessing methods before feeding the input image to the model. NVIDIA researchers introduce their preprocessing methods in the paper [3], including cropping, resizing, and RGB to YUV.

C. Online Attacks and Offline Attacks

Prior research primarily focuses on offline attacks against classification models, while we investigate online attacks against regression models.

Offline attacks apply perturbations to static images. Under the scenario of autonomous driving, an offline attack splits the driving record into static images and corresponding steering angles. The perturbation is applied to each static image, and then the attack is evaluated using the overall success rate [12].

Online attacks apply perturbation in a dynamic environment. Rather than apply the perturbation to static images in a driving record, we deploy the perturbation while the vehicle is driving. Thus, we can investigate the driving models' reactions to the attacks.

The difference between online and offline attacks is that the ground truth y^* is unavailable for online attacks. For autonomous driving, offline attacks take pre-recorded human drivers' steering angles as the ground truth, while real-time online attacks do not have access to pre-recorded human decisions. We use the model output $\hat{y} = f(\theta, x)$ as the ground truth because we assume that the driving model is accurate enough. Our assumption is reasonable because if the model is inaccurate, we do not need to attack the system in the first place. The erroneous model is already a threat to the driving task.

Since it is risky to perform online attacks against real-world autonomous driving systems, we tested our attacks in self-driving simulators and a Turtlebot. We devised an image-specific strong attack and an image-agnostic stealth attack that could manipulate the behavior of end-to-end autonomous driving systems.

D. Image-specific Strong Attack

The first adversarial attack against a classifier [4] is an image-specific attack that generates one perturbation for every input image. Instead of minimizing the training loss $J(\hat{y}, y^*)$, Goodfellow et al. maximize the training loss and then use the gradient of the training loss over the input to generate the perturbation.

However, online attacks do not have access to the ground truth y^* , thus the training loss $J(\hat{y}, y^*)$ cannot be calculated. As a result, we need a new adversarial loss $J(\hat{y})$ that only requires the model output \hat{y} to generate the perturbation.

To attack a regression model, we notice that we can either increase or decrease the output. For example, to attack the end-to-end driving regression model, we can either deviate the vehicle to the left by decreasing the output or to the right by increasing the output. As a result, attacking regression models is a special case of attacking classification models, where we have only two choices: increasing or decreasing.

Intuitively, we devise a very straightforward adversarial loss functions for the image-specific attack.

$$J'_{\text{left}}(\hat{y}) = -\hat{y} \quad (2)$$

$$J'_{\text{right}}(\hat{y}) = \hat{y} \quad (3)$$

Algorithm 1 Image-specific Strong Attack

Input: The regression model $f(\theta, x)$, the input image x_t at time step t .

Parameters: the strength of the attack ϵ measured by l_{inf} norm.

Output: Image-specific perturbation η .

for each time step t **do**

Inference: $\hat{y} = f(\theta, x)$

Gradients: $\nabla = \frac{\partial J'(\hat{y})}{\partial x'}$

Perturbation: $\eta = \epsilon \text{sign}(\nabla)$

end for

Algorithm 2 Image-agnostic Stealth Attack (Training)

Input: The regression model $f(\theta, x)$, input images in a driving record X , the target direction $I \in \{-1, 1\}$.

Parameters: the number of iterations n , the learning rate α , the step size ξ , and the strength of the attack ϵ measured by l_{∞} norm.

Output: Image-agnostic perturbation η .

Initialization: $\eta \leftarrow 0$

for each iteration **do**

for each input image x in the driving record X **do**

Inference: $\hat{y} = f(\theta, x + \eta)$

if $\text{sign}(\hat{y}) \neq I$ **then**

$x' = x + \eta$

$\eta_t \leftarrow 0$

while $\text{sign}(\hat{y}) \neq I$ **do**

Gradients: $\nabla = \frac{\partial J'(\hat{y})}{\partial x'}$

Perturbation: $\eta_t = \eta_t + \text{proj}_2(\nabla, \xi)$

Inference: $\hat{y} = f(\theta, x + \eta_t)$

end while

$\eta = \text{proj}_{\infty}(\eta + \frac{\alpha}{\xi} \eta_t, \epsilon)$

end if

end for

end for

Then we can generate the perturbation similar to the Fast Gradient Sign Method (FGSM). The ϵ is a scaling factor that decides the visibility of the perturbation.

$$\eta = \epsilon \text{sign}[\nabla_x(J'(\hat{y}))] \quad (4)$$

For example, if the attacker wishes to attack the vehicle to the right side (steering angle > 0), the objective is to increase the model output. We can use the adversarial loss $J'_{\text{right}}(\hat{y})$ to generate the perturbation. $\nabla_x(J'(\hat{y}))$ represents the gradient of the adversarial loss over the input. The gradient gives us the information if the adversarial loss \hat{y} increases, how will the change back-propagates to the input. We summarize the image-specific attack in Algorithm 1.

Our experimental results show that the image-specific attack is a strong attack that deviates the vehicle to the outside of the lane in several seconds.

E. Image-agnostic Stealth Attack

Minor mistakes at some critical points could also cause traffic accidents. For example, decreasing the steering angle by a little bit may result in failing to steer around sharp corners. Thus, stealth attacks with a low overall success rate could still be perilous at some points. Besides, the image-specific attack largely deviates the steering angle in a short period, making it inconspicuous. Hence we introduce another stealth white-box attack that generates a universal adversarial perturbation (UAP) [13] to attack all input images at different time steps.

The image-agnostic stealth attack combines the idea of DeepFool [14] and Projected Gradient Descent (PGD) [15]. The attack consists of two procedures, the training, and the deployment. We first train a universal adversarial perturbation (UAP) online or via a driving record and then deploy the UAP.

The Training: We first decide our target direction that either attacks the vehicle to the left side ($\hat{y} < 0$) or to the right side ($\hat{y} > 0$), and then choose the corresponding adversarial loss function ($J'_{left}(\hat{y})$ or $J'_{right}(\hat{y})$). the perturbation is initialized with zero. For each input image at each timestep, if the direction of the model output is not the same as the desired direction, we find the minimum perturbation that changes the sign of the model output to the desired direction.

To change the direction of the model output, we calculate the gradient of the adversarial loss $J'(\hat{y})$ and then project the gradient to the L_2 ball to get the minimum perturbation. The close form solution of the optimization problem $argmin ||x - y||_2$ with the constraint $||x|| \leq \xi$ is given by Convex Optimization which is proofed via Lagrangian and KKT conditions.

$$\underset{\eta'}{argmin} ||\eta - \eta'||_2 \text{ subject to } ||\eta'\|_2 \leq \xi \quad (5)$$

$$\Delta\eta_t = proj_2(\eta, \xi) = \xi \frac{\nabla_x[J'(\hat{y})]}{||\nabla_x[J'(\hat{y})]||_2} \quad (6)$$

After applying the temporary perturbation η_t at timestep t , if the direction of the model output matches the desired direction, we incorporate the temporary perturbation η_t to the overall perturbation η and then project η on the l_2 ball centred at 0 and of radius ϵ to ensure the constraint $||\eta'\|_2 \leq \epsilon$ is satisfied. We summarize the attack in Algorithm 2.

The strength of the attack is not as strong as the image-specific attack, but it still adds an opposite force to the vehicle while turning through the corner.

F. System Architecture

The Robot Operating System (ROS) [16] is the most popular software framework in robotic research and applications. Dieber et al. propose the Stealth Publisher Attack that injects malicious data into a running ROS application [17]. We can exploit the same vulnerability to inject the adversarial perturbation into a running end-to-end driving ROS application.

We design an adversarial driving system to attack the end-to-end autonomous driving system. The system consists of three key components: the simulator, the server, and the Web User Interface (UI).

Simulator: The simulator publishes the image captured by the front camera to the server. Meanwhile, it accepts steering commands from the server to manipulate the vehicle. The modular design pattern enables us to replace the simulator with a real Turtlebot without breaking the whole system.

Server: The server receives input images from the simulator via WebSocket connections and then sends back the control commands. Meanwhile, it receives attack commands from the web browser and then injects the adversarial perturbation into the input image. Besides, the end-to-end driving model is deployed on the server as well.

The Web UI: We use a website as a front end where the attacker can monitor the status of the simulator and choose different attacks.

We trained three models in three different environments to validate our attacks, and we present our experimental results in the next section.

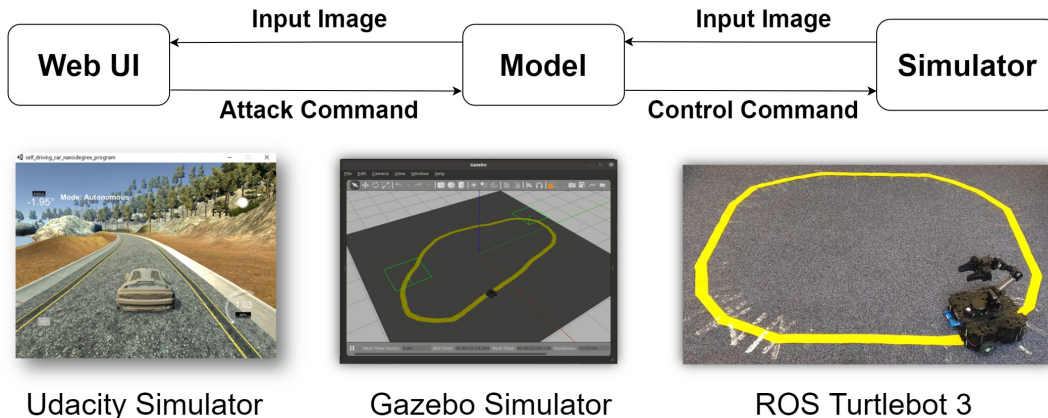


Fig. 2: The architecture of the Adversarial Driving System. We tested our attacks in three environments: the Udacity Simulator, the ROS Gazebo Simulator, and a real Turtlebot 3.

IV. EXPERIMENTAL RESULTS

A. Model Training

Our objective is to achieve real-time online attacks against the end-to-end imitation learning model. The target imitation learning models were trained from human driving records. In total, we collected 32k images of human driving records in our test environments: the Udacity Simulator (8k), the Gazebo Simulator (12k), and a real Turtlebot 3 (12k). Then we trained three end-to-end driving models respectively.

Our experiment showed that all three models in different environments were vulnerable to adversarial attacks. In the following sections, we choose data from the Udacity Simulator to analyze the attack because it is easier to reproduce and examine for other researchers.

B. The Image-Specific Strong Attack

We first demonstrate that random noises do not threaten the end-to-end driving model. We can vary the strength of the image-specific attack by changing ϵ . The image-specific attack adds ϵ or minus ϵ to each pixel based on the sign of the gradient. Thus we construct a random noise that randomly adds or minus ϵ to each pixel.

In Figure 4, we applied three different attacks that are of the same strength. Once under the image-specific attack, the vehicle drove off the road in several seconds.

Furthermore, we measured the absolute change of steering angle on average over 800 attacks (see Table II). Even the weakest image-specific attack ($\epsilon = 0.1$) is much stronger than the strongest random noises ($\epsilon = 8$). When $\epsilon = 4$ and $\epsilon = 8$, we can even deviate the steering angle outside the range of $[-1, 1]$.

| Attack Strength | Random Noises | Image-Specific Attack |
|------------------|---------------|-----------------------|
| $\epsilon = 0.1$ | 0.0002 | 0.1448 |
| $\epsilon = 1$ | 0.0020 | 0.4779 |
| $\epsilon = 2$ | 0.0048 | 0.7329 |
| $\epsilon = 4$ | 0.0150 | 1.4895 |
| $\epsilon = 8$ | 0.0278 | 2.4469 |

TABLE II: The average of the absolute steering angle change under 800 image-specific attacks.

As a result, the image-specific attack is very strong, but its strength is also its weakness. To produce such a strong perturbation, it needs to calculate the gradients of each input image. Under a real-world scenario, we may not have access to the input image and gradients. Thus, we devise the image-agnostic attack that trains the perturbation using driving records and does not need access to the input and gradients during the deployment.

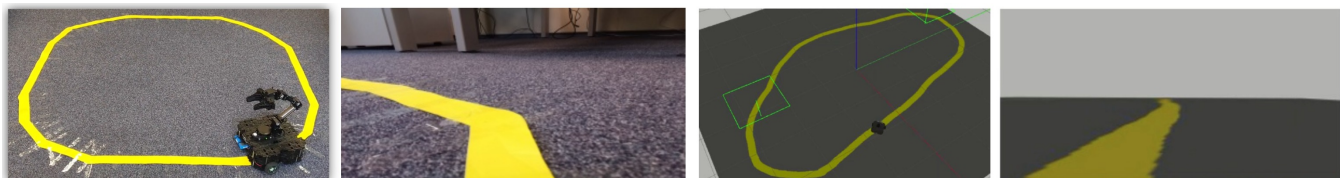
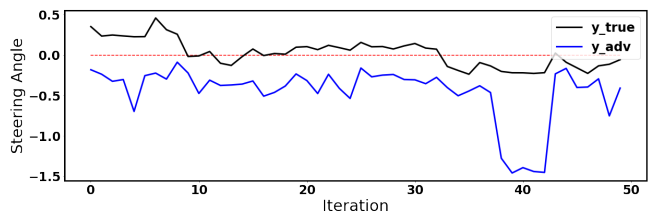
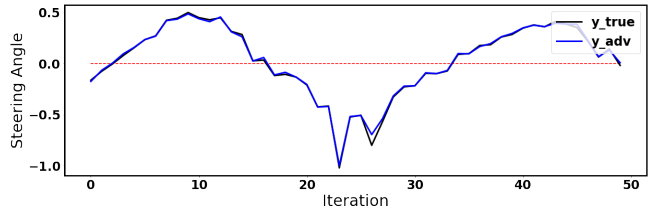


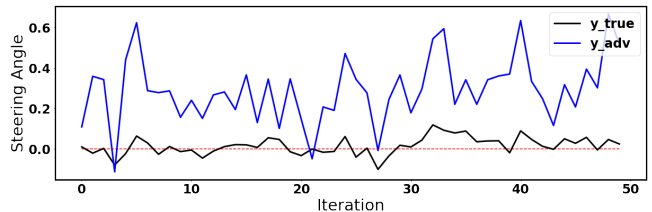
Fig. 3: Our test platforms and input images in ROS: A real turtlebot and ROS Gazebo Simulator.



(a) The image-specific Left Attack deviates the vehicle to the left by decreasing the steering angle, thus the y_{adv} is smaller than y_{true} .



(b) The random noises barely deviates y_{adv} from y_{true} .



(c) The image-specific Right Attack deviates the vehicle to the right by increasing the steering angle, thus the y_{adv} is greater than y_{true} .

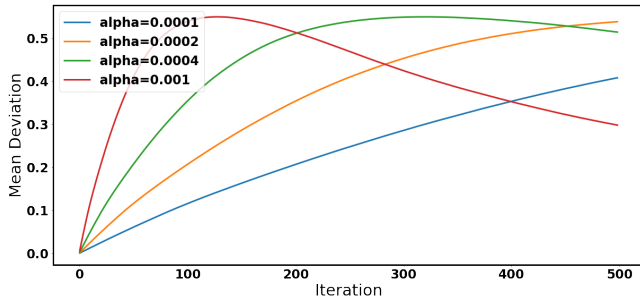
Fig. 4: The Image-Specific attack and random noises with the same strength ($\epsilon = 1$).

C. The Image-Agnostic Stealthy Attack

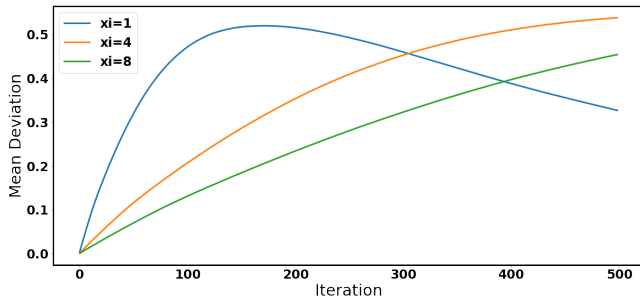
Similarly, we compared the strength of image-agnostic attacks with random noises to demonstrate the efficacy of the attack. Though the image-agnostic attack is weaker than the image-specific attack, it is still stronger than random noises (see Table III).

| Attack Strength | Random Noises | Image-Agnostic Attack |
|------------------|---------------|-----------------------|
| $\epsilon = 0.1$ | 0.0002 | 0.0373 |
| $\epsilon = 1$ | 0.0020 | 0.1109 |
| $\epsilon = 2$ | 0.0048 | 0.1294 |
| $\epsilon = 4$ | 0.0150 | 0.1131 |
| $\epsilon = 8$ | 0.0278 | 0.1275 |

TABLE III: The average of the absolute steering angle change under 800 image-agnostic attacks ($\alpha = 0.002$, $\xi = 4$, $n = 500$).



(a) The learning rate α controls the variation of the perturbation during the whole iteration. We tested different α with fixed $\epsilon = 1, \xi = 4$. As α increases, the iteration is faster, but the iteration process becomes stochastic, and the mean deviation decreases after 100 steps when $\alpha > 0.01$.



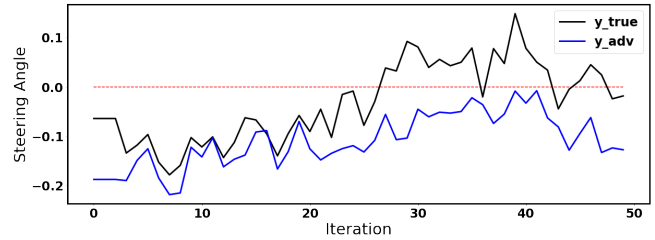
(b) The step size ξ decides how fast the perturbation updates to change the model output to the desired direction for each input image x . A smaller ξ makes the update towards the target direction more steady, but the iteration takes more time. A larger ξ can change the direction of the model output in a single step, but the perturbation may not generalize well to other inputs.

Fig. 5: The mean absolute deviation of the steering angle during the training process with different hyper-parameters.

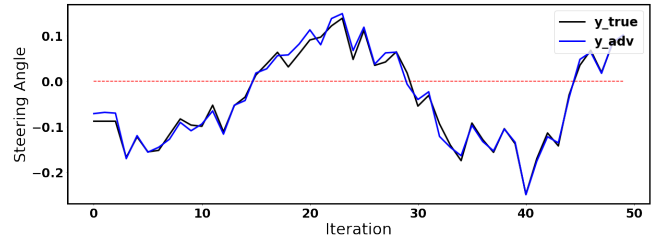
Our experimental results in Table III showed that the strength of the image-agnostic attack did not improve after $\epsilon > 2$ because there is a limitation on the generalizability of the perturbation. The perturbation could increase the model output for some inputs but may decrease when the vehicle drives to other locations. Increasing ϵ adds more variations to the model prediction while the average absolute deviation remains stable.

We further investigated the effect of the learning rate α and the step size ξ on the training process (see Figure 6), and our experiments showed that $\alpha = 0.0002, \xi = 4$ could generate an image-agnostic perturbations with $\epsilon = 1$ that is comparable to the image-agnostic attack with $\epsilon = 0.1$.

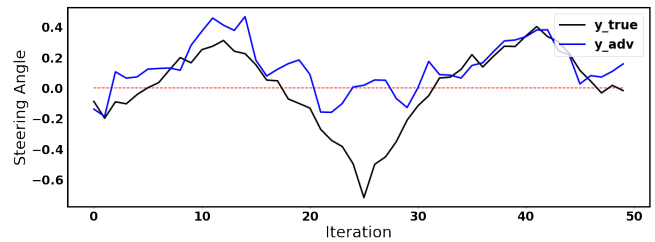
As a result, the image-agnostic perturbation is stealthy because the strength of the attack is less noticeable than the image-specific attack. However, the image-agnostic attack makes the vehicle difficult to control at sharp corners, which could lead to incidents at some critical points. Besides, the image-agnostic attack applies the same perturbation to all frames. Thus, the deployment of the image-agnostic attack is much faster than the image-specific attack.



(a) The image-agnostic Left Attack decreases the model output ($y_{adv} < 0$), making it difficult to turn right. ($\epsilon = 1$)



(b) The random noises barely deviates y_{adv} from y_{true} .



(c) The image-agnostic Right Attack increases the model output ($y_{adv} > 0$), making it difficult to turn left. ($\epsilon = 1$)

Fig. 6: The Image-Agnostic attack ($\alpha = 0.002, \xi = 4, n = 500$) and random noises with the same strength ($\epsilon = 1$).

V. CONCLUSIONS

In conclusion, this research demonstrates that it is possible to attack the end-to-end driving model in real-time. We devise a strong image-specific attack and a stealthy image-agnostic attack. Though the mean absolute deviation of the image-agnostic attack is smaller than the image-specific attack, both attacks are more effective than random noises. The image-agnostic attack deviates the vehicle to the outside of the lane in several seconds, while the image-agnostic attack could cause incidents at sharp corners.

For safety-critical robotic applications, it is possible to inject the adversarial perturbation into relevant ROS topics and thus fool end-to-end deep learning models. As a result, we may pause and ponder over the safety of end-to-end models in safety-critical applications.

ACKNOWLEDGMENT

The project is supported by Offshore Robotics for Certification of Assets (ORCA) Partnership Resource Fund (PRF) on Towards the Accountable and Explainable Learning-enabled Autonomous Robotic Systems (AELARS) [EP/R026173/1].

REFERENCES

- [1] A. Dosovitskiy, G. Ros, F. Codevilla, A. Lopez, and V. Koltun, "CARLA: An open urban driving simulator," in *Proceedings of the 1st Annual Conference on Robot Learning*, 2017, pp. 1–16.
- [2] S. Shah, D. Dey, C. Lovett, and A. Kapoor, "Airsim: High-fidelity visual and physical simulation for autonomous vehicles," in *Field and Service Robotics*, 2017.
- [3] M. Bojarski, D. Del Testa, D. Dworakowski, B. Firner, B. Flepp, P. Goyal, L. D. Jackel, M. Monfort, U. Muller, J. Zhang, *et al.*, "End to end learning for self-driving cars," *arXiv preprint arXiv:1604.07316*, 2016.
- [4] I. J. Goodfellow, J. Shlens, and C. Szegedy, "Explaining and harnessing adversarial examples," *arXiv preprint arXiv:1412.6572*, 2014.
- [5] E. Yurtsever, J. Lambert, A. Carballo, and K. Takeda, "A Survey of Autonomous Driving: Common Practices and Emerging Technologies," *IEEE Access*, vol. 8, pp. 58 443–58 469, 2020.
- [6] A. Tampuu, T. Matiisen, M. Semkin, D. Fishman, and N. Muhammad, "A survey of end-to-end driving: Architectures and training methods," *IEEE Transactions on Neural Networks and Learning Systems*, 2020.
- [7] D. A. Pomerleau, "Alvinn: An autonomous land vehicle in a neural network," in *Advances in Neural Information Processing Systems*, D. Touretzky, Ed., vol. 1. Morgan-Kaufmann, 1989.
- [8] U. Muller, J. Ben, E. Cosatto, B. Flepp, and Y. Cun, "Off-road obstacle avoidance through end-to-end learning," in *Advances in Neural Information Processing Systems*, Y. Weiss, B. Schölkopf, and J. Platt, Eds., vol. 18. MIT Press, 2006.
- [9] K. Ren, T. Zheng, Z. Qin, and X. Liu, "Adversarial attacks and defenses in deep learning," *Engineering*, vol. 6, no. 3, pp. 346–360, 2020.
- [10] S. Villar, D. W. Hogg, N. Huang, Z. Martin, S. Wang, and G. Scanlon, "Adversarial attacks against linear and deep-learning regressions in astronomy," in *Proceedings of Machine Learning Research 2020 1st Annual Conference on Mathematical and Scientific Machine Learning*. Mathematical and Scientific Machine Learning Conference, 2019.
- [11] A. T. Nguyen and E. Raff, "Adversarial attacks, regression, and numerical stability regularization," *arXiv preprint arXiv:1812.02885*, 2018.
- [12] Y. Deng, X. Zheng, T. Zhang, C. Chen, G. Lou, and M. Kim, "An analysis of adversarial attacks and defenses on autonomous driving models," in *2020 IEEE International Conference on Pervasive Computing and Communications (PerCom)*. IEEE, 2020, pp. 1–10.
- [13] S.-M. Moosavi-Dezfooli, A. Fawzi, O. Fawzi, and P. Frossard, "Universal adversarial perturbations," in *Proceedings of the IEEE conference on computer vision and pattern recognition*, 2017, pp. 1765–1773.
- [14] S.-M. Moosavi-Dezfooli, A. Fawzi, and P. Frossard, "Deepfool: a simple and accurate method to fool deep neural networks," in *Proceedings of the IEEE conference on computer vision and pattern recognition*, 2016, pp. 2574–2582.
- [15] A. Madry, A. Makelov, L. Schmidt, D. Tsipras, and A. Vladu, "Towards deep learning models resistant to adversarial attacks," *arXiv preprint arXiv:1706.06083*, 2017.
- [16] S. Macenski, T. Foote, B. Gerkey, C. Lalancette, and W. Woodall, "Robot operating system 2: Design, architecture, and uses in the wild," *Science Robotics*, vol. 7, no. 66, p. eabm6074, 2022.
- [17] B. Dieber, R. White, S. Taurer, B. Breiling, G. Caiazza, H. Christensen, and A. Cortesi, "Penetration testing ros," in *Robot operating system (ROS)*. Springer, 2020, pp. 183–225.